

Control of Luminescence Decay and Flavin Binding by the LuxA Carboxyl-Terminal Regions in Chimeric Bacterial Luciferases[†]

Nelly Valkova, Rose Szittner, and Edward A. Meighen*

Department of Biochemistry, McGill University, 3655 Drummond Street, Montreal, Quebec, H3G 1Y6, Canada

Received June 18, 1999; Revised Manuscript Received August 5, 1999

ABSTRACT: Bacterial luciferases (LuxAB) can be readily classed as slow or fast decay luciferases based on their rates of luminescence decay in a single turnover assay. Luciferases from *Vibrio harveyi* and *Xenorhabdus* (*Photorhabdus*) *luminescens* have slow decay rates, and those from the *Photobacterium* genus, such as *P. (Vibrio) fischeri*, *P. phosphoreum*, and *P. leiognathi*, have rapid decay rates. By generation of an *X. luminescens*-based chimeric luciferase with a 67 amino acid substitution from *P. phosphoreum* LuxA in the central region of the LuxA subunit, the “slow” *X. luminescens* luciferase was converted into a chimeric luciferase, LuxA₁B, with a significantly more rapid decay rate. Two other chimeras with *P. phosphoreum* sequences substituted closer to the carboxyl terminal of LuxA, LuxA₂B and LuxA₃B, retained the characteristic slow decay rates of *X. luminescens* luciferase but had weaker interactions with both reduced and oxidized flavins, implicating the carboxyl-terminal regions in flavin binding. The dependence of the luminescence decay on concentration and type of fatty aldehyde indicated that the decay rate of “fast” luciferases arose due to a high dissociation constant (K_a) for aldehyde (A) coupled with the rapid decay of the resultant aldehyde-free complex via a dark pathway. The decay rate of luminescence (k_T) was related to the decanal concentration by the equation: $k_T = (k_L A + k_D K_a)/(K_a + A)$, showing that the rate constant for luminescence decay is equal to the decay rate via the dark- (k_D) and light-emitting (k_L) pathways at low and high aldehyde concentrations, respectively. These results strongly implicate the central region in LuxA₁B as critical in differentiating between “slow” and “fast” luciferases and show that this distinction is primarily due to differences in aldehyde affinity and in the decomposition of the luciferase–flavin–oxygen intermediate.

Bacterial luciferases catalyze the concomitant oxidation of reduced flavin mononucleotide (FMNH₂)¹ and a long-chain aldehyde into FMN and the corresponding long-chain fatty acid (1). This reaction, shown in Figure 1, is dependent on the sequential formation of several enzyme–flavin intermediates. Luciferase (E) interacts with FMNH₂ (FH₂) to form the EFH₂ complex which subsequently reacts with O₂ to yield an oxygenated enzyme–flavin complex, EFH₂O₂ (EFO). This complex can either decompose by a dark side pathway with a rate constant k_D to yield oxidized FMN (F) and H₂O₂, or interact with aldehyde (RCOH) to form an EFH₂O₂–RCOH complex (EFOA). Decay of EFOA can occur by dissociation of the aldehyde followed by decomposition via the dark pathway, or the reaction goes to completion with the emission of blue–green light at 490 nm characterized by the rate constant k_L . The standard luciferase assay is quite unusual in that the enzyme undergoes only a single turnover as the FMNH₂ substrate is oxidized chemically at a rate faster than the decay of the EFOA intermediate (2). Consequently, light rises to a maximum in the first

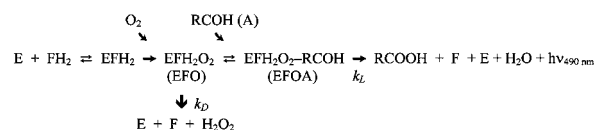


FIGURE 1: Intermediates in the bacterial luciferase reaction. Reduced flavin mononucleotide (FH₂) reversibly binds to the enzyme (E) to form an EFH₂ complex. In the presence of molecular oxygen (O₂), an enzyme–flavin oxygenated intermediate, EFH₂O₂ (EFO), is formed, which can dissociate in a dark reaction to oxidized flavin mononucleotide (F) and H₂O₂ or bind a long-chain aldehyde RCOH (A), to produce the EFH₂O₂–RCOH (EFOA) complex. The products FMN (F) and fatty acid (RCOOH) are generated after conversion of the EFOA intermediate into light.

second of the assay and then decreases exponentially with the loss of the EFOA complex at a rate dependent on the specific luciferase and aldehyde.

The three-dimensional structure of *Vibrio harveyi* bacterial luciferase has been recently solved at a resolution of 1.5 Å (3). Each subunit of the heterodimeric (LuxAB) enzyme forms an (α/β)₈ barrel motif. The two noncovalently bound subunits interface by means of two α -helices in the amino-terminal half of each subunit to form a parallel four-helix bundle. As the enzyme was crystallized without bound substrates, only inferences can be made with regard to the crucial residues involved in catalysis. A mobile region located in the LuxA subunit (4) appears to be important, as substrates protect this region from proteolytic cleavage (5). Two tryptophan residues adjacent to this mobile loop and

[†] Supported by Grant MT4314 from the Medical Research Council of Canada.

* To whom correspondence should be addressed. Phone: +1 514 398 7272. Fax: +1 514 398 7384. E-mail: meighen@med.mcgill.ca.

¹ Abbreviations: FMN, flavin mononucleotide; FMNH₂, reduced FMN; XL, *Xenorhabdus luminescens*; PP, *Photobacterium phosphoreum*; PL, *Photobacterium leiognathi*; LU, light unit.

in close proximity to each other, Trp194 and Trp250, have also been implicated in activity and/or flavin binding (6). Based on a strong electron density peak in LuxA believed to arise from a phosphate or sulfate anion bound during crystallization, the flavin ring of FMNH₂ was modeled to the interface between these tryptophans by positioning the phosphate moiety of FMNH₂ at this electron-dense site (4). However, the specific locations of the aldehyde and flavin binding sites remain unknown, although it is likely that they are bound near the carboxyl terminus of LuxA based on the location of the active sites of other (α/β)₈ barrel enzymes (7).

A large difference in the luminescence decay rates has been used as a taxonomic basis to class luminescent bacteria into two clearly distinct groups (8, 9). Over 3000 strains of luminescent bacteria from the *Vibrio* and *Photobacterium* genera could be classed as containing luciferases either with a slow or with a fast decay of luminescence. The luminescent species with "slow" luciferases were all *Vibrio harveyi* strains while *Photobacterium* (*Vibrio*) *fischeri*, *P. phosphoreum*, and *P. leiognathi* species all contained "fast" luciferases. More recent characterization of strains of the terrestrial luminescent bacterium *Xenorhabdus* (*Photorhabdus*) *luminescens* has shown that this species contains a luciferase with a slower decay than that of *V. harveyi* luciferase (10–12). Hence, bacterial luciferases can be classed into two distinct categories based on their luminescence decay rates.

The study of chimeric enzymes has previously proven instrumental in delineating regions crucial in catalysis (13–16), although the interchange of specific domains of closely related enzymes may result in instability or insolubility of the resultant chimera, as observed for chimeras of ornithine and aspartate transcarbamoylases (17). In bacterial luciferase, the LuxA subunit is believed to control the primary kinetic properties of luciferase (18, 19). Luciferases containing chimeric LuxA subunits thus have the potential to define key regions involved in luminescence. An important first step toward characterizing the active site rests with the identification of the region responsible for the classification of luciferases as "slow" or "fast" based on their decay rates. Since a disruption of the interactions between the amino-terminal halves of the LuxA and LuxB subunits (3, 4) would prevent the generation of an efficient and functional enzyme (19, 20), a set of chimeric luciferases containing portions of the carboxyl-terminal half of XL LuxA were replaced with the corresponding sequences from PP LuxA. Remarkably, a chimera containing a replacement of 17% of its LuxA sequence with that of PP luciferase was converted from a "slow" XL luciferase to a luciferase with properties more similar to PP luciferase, including a rapid luminescence decay rate and a decreased thermal stability. Analysis of the decay rates as a function of decanal concentration indicated that the molecular basis for the fast decay of luminescence arose primarily due to a preferential decay of the EFOA intermediate via the dark pathway and not to a more rapid conversion into light. Two other XL-based LuxAB chimeras containing PP segments of comparable length had weaker flavin interactions but remained "slow" luciferases with properties more closely related to the parental XL LuxAB.

MATERIALS AND METHODS

Chemicals. Flavin mononucleotide (FMN) was a gift from Sigma and used without further purification. Reduced flavin mononucleotide (FMNH₂) was produced by bubbling H₂ through a 50 μ M FMN solution in the presence of a Pt catalyst (Fluka). The flavin analogue ω -carboxypentylflavin was originally a gift from Dr. D. B. McCormick (Cornell University, New York). The phosphate buffers were prepared by mixing appropriate amounts of NaH₂PO₄ and K₂HPO₄ obtained from Baker. The concentrations of flavins were determined from their absorbance at 450 nm using an extinction coefficient of 12 200 M⁻¹ cm⁻¹. Sodium hydro-sulfite was purchased from Fisher. Sodium sulfate was purchased from Anachemia. All aliphatic aldehydes were obtained from Aldrich, and myristic acid was purchased from Sigma. Bovine serum albumin (BSA) was purchased from Sigma or from Boehringer Mannheim. All compounds were reagent grade.

Construction of Chimeric and Hybrid Luciferases. Chimeric luciferases were generated by insertion of unique restriction sites into *X. luminescens luxA* followed by insertion of the homologous region of *P. phosphoreum luxA* flanked by the corresponding restriction sites. Initially, a unique *Xba*I site was introduced into the middle of *luxA* in a pT7-5 plasmid containing the XL *luxAB* genes separated by a unique *Bam*HI site and flanked upstream and downstream by unique *Eco*RI and *Pst*I sites, respectively (see Figure 2 under Results). This was accomplished by ligation of the pT7-5 plasmid extending from *Eco*RI to *Pst*I (or *Bam*HI) with two PCR fragments simultaneously, one extending from the *Xba*I site upstream to *Eco*RI and one downstream to the *Pst*I (or *Bam*HI) site. Unique *Sal*I and *Kpn*I sites were then introduced sequentially in *luxA* between the *Xba*I and *Bam*HI sites using the same approach. Custom-designed primers used for PCR were from Gibco-BRL. Introduction of the restriction sites resulted in a single amino acid change in sequence at the *Xba*I site (Tyr to Gly) with no changes at the *Sal*I and *Kpn*I sites. Part of *luxA* was then excised from the resultant plasmid by the appropriate pair of restriction enzymes (i.e., *Xba*I and *Sal*I; *Sal*I and *Kpn*I; *Kpn*I and *Bam*HI), the homologous region in PP *luxA* copied by PCR using primers flanked by the corresponding restriction sites, and the PP *luxA* ligated into the excised pT7-5 plasmid with XL *luxB* and the remainder of XL *luxA*. The generation of chimeric *luxA* genes was extremely efficient since only complete constructs emitted light after transformation into *E. coli*; restriction analysis was then used to confirm the presence of PP *lux* DNA. Hybrid chimeras containing PP *luxB* and *P. leiognathi luxB* were generated by PCR of the corresponding *luxB* genes with primers containing flanking *Bam*HI and *Pst*I sites followed by ligation into the plasmid with the chimeric or parental *luxAB* genes with the XL *luxB* excised by restriction with *Bam*HI and *Pst*I.

Expression and Enzyme Purification. Each of the pT7-5 plasmids containing hybrid, chimeric, or parental *luxAB* genes were transformed into *E. coli* strain K38 containing the plasmid pGP1-2 coding for the T7 promoter–RNA polymerase expression system as previously described (11, 21). The cells were grown in the appropriate media with 50 μ g/mL ampicillin and 40 μ g/mL kanamycin to an OD_{660nm} of 2.5–2.8 at 30 \pm 2 $^{\circ}$ C, centrifuged, and suspended in 10%

of the original culture volume of 50 mM phosphate buffer, pH 7.0, and 20 mM β -mercaptoethanol before lysis by ultrasonication. For luciferases with low activity, the cells were suspended in 1% of the original culture volume before lysis. Purification was performed according to the method of Gunsalus-Miguel et al. (22).

The protein concentration was determined from the absorbance at 280 nm using molar extinction coefficients of $8.8 \times 10^4 \text{ M}^{-1} \text{ cm}^{-1}$ for XL and $7.2 \times 10^4 \text{ M}^{-1} \text{ cm}^{-1}$ for PP luciferase, $8.7 \times 10^4 \text{ M}^{-1} \text{ cm}^{-1}$ for the LuxA₂B chimera, and $8.5 \times 10^4 \text{ M}^{-1} \text{ cm}^{-1}$ for the LuxA₃B chimera calculated on the basis of the number of tryptophans and tyrosines present in each protein. The molecular weights calculated based on the proteins' sequences were 7.9×10^4 for XL luciferase and 7.8×10^4 for PP luciferase and the chimeric luciferases. The purified native and chimeric luciferases had 95% or greater purity as determined from SDS gel electrophoresis. The enzymes were kept in storage at -20°C in the presence of 20 mM β -mercaptoethanol and 30% glycerol.

Luminescence Assays. Two types of in vitro luminescence assays were performed. The first assay, referred to as the standard flavin injection assay, consists of the rapid injection of 1 mL of 50 μM catalytically reduced FMNH₂ into a 1 mL mixture containing the luciferase and 0.001% aldehyde dispersion in 50 mM phosphate buffer, pH 7.0, and 0.2% bovine serum albumin (BSA). The second assay, known as the dithionite assay (18), consists of the rapid injection of 1 mL of a 0.01% aldehyde suspension in 50 mM phosphate buffer, pH 7.0, into a 1 mL mixture containing the luciferase and 50 μM FMNH₂ kept reduced by the presence of 2 mM sodium hydrosulfite and buffered with 50 mM phosphate buffer, pH 7.0, and 20 mM β -mercaptoethanol. Dithionite assays showing stimulation of luminescence by sulfate ions were performed by adding the required amount of dianion into a 1 mL luciferase-riboflavin mixture except only 10 mM phosphate was used as buffer. The decay rate of the hydroperoxyflavin intermediate was determined by injecting 1 mL of catalytically reduced FMNH₂ into a 1 mL solution containing luciferase in 50 mM phosphate buffer, pH 7.0, and 0.2% BSA, followed by a timed injection of 1 mL of 0.001% decanal in 50 mM phosphate buffer, pH 7.0.

All luminescence assays were conducted at room temperature ($23 \pm 2^\circ \text{C}$). The rate of luminescence decay was determined from the time elapsed between 80% and 40% of the maximum light intensity. Specific activities of the luciferases were expressed as LU/mg. One LU is equivalent to 3.6×10^9 quanta s^{-1} based on the light standard of Hastings and Weber (23). In vivo luminescence in *E. coli* cells was measured immediately after vortexing 1 μL of neat decanal into 1 mL of cell culture. The light intensity was measured on a custom-built luminometer equipped with an XY recorder with a built-in time base.

Steady-State Fluorescence Measurements. Fluorescence studies were performed on a Hitachi F-3010 fluorometer equipped with a 150 W xenon short-arc lamp and a 5 mm path length quartz cuvette. The wavelength dispersion was 3 nm for excitation and 5 nm for emission, and the excitation wavelength was 296 nm. The samples were incubated in 50 mM phosphate buffer, pH 7.0, and 20 mM β -mercaptoethanol at $25 \pm 0.2^\circ \text{C}$. The determination of the dissociation constant for FMN was determined from decreases in the intrinsic protein fluorescence, monitored at 340 nm, upon

binding of FMN. The observed fluorescence was corrected for changes in sample volume and subtracted from the base line fluorescence of the buffer. As well, the fluorescence was corrected for the inner filter effect caused by the competitive absorption by FMN according to the equation (24):

$$F(\lambda)_{\text{Corr}} = F(\lambda)_{\text{Obs}} \text{antilog}[\text{OD}_{\text{Ex}}(\lambda)/2 + \text{OD}_{\text{Em}}(\lambda)/2]$$

where $\text{OD}_{\text{Ex}}(\lambda)$ represents the optical density of the sample at the excitation wavelength and $\text{OD}_{\text{Em}}(\lambda)$ the optical density of FMN at the emission wavelength.

RESULTS

Construction and Structure of Chimeric Luciferases. The composition, amino acid sequence, and structure of three chimeras of LuxA are given in Figure 2. Approximately one-sixth of the sequence of the *luxA* gene of *X. luminescens* has been replaced with the homologous region of PP *luxA* (LuxA₁B, LuxA₂B, and LuxA₃B) in each chimera (Figure 2A). Substitution with PP DNA was accomplished by inserting three unique restriction sites, *Xba*I, *Sal*I, and *Kpn*I, in the *luxA* gene at approximately equal intervals in the last half of the gene so that the corresponding DNA fragments from PP *luxA* could be transferred. Alignment of the sequences in the carboxyl-terminal half of LuxA shows that 32 of 68 residues (47%) replaced in LuxA₁B, 23 of 68 residues (34%) replaced in LuxA₂B, and 18 of the 52 residues (35%) replaced in LuxA₃B were different than those present in the parent XL luciferase (Figure 2B).

The three-dimensional crystal structure of *V. harveyi* luciferase, which has 85% sequence identity to XL luciferase, and thus can serve as a structural model for the XL-based chimeras, is shown in Figure 2C to illustrate the substituted portions in LuxA₁B (yellow), LuxA₂B (green), and LuxA₃B (red). The region replaced in LuxA₁B includes three β -strands (β_5 , β_6 , and β_7) and two α -helices (α_5 and α_6) while that in LuxA₂B includes the protease-sensitive loop flanked by two α -helices (α_{7a} and α_{7b}) and a small three-residue β -strand (β_{7a}). The modified region in LuxA₃B comprises two α -helices (α_7 and α_8) flanking a five-residue β -strand (β_8). In both LuxA₂B and LuxA₃B, the modified regions are located on the periphery of the upper portion of LuxA, well separated from contact with LuxB, while the substituted β -strands in LuxA₁B extend into the inner portion of LuxA.

In Vivo Luminescence of Chimeric Constructs. Table 1 gives the in vivo luminescence of *E. coli* cells expressing the different hybrid and chimeric luciferases relative to that of the parent XL luciferase (LuxAB). *E. coli* cells containing the chimeras LuxA₂B and LuxA₃B have 31% and 9%, respectively, of the light intensity of *E. coli* cells with the parental luciferase while cells with LuxA₁B had very low light emission (0.03%). Activity could not be detected in a chimera with all three regions replaced with PP luciferase (LuxA₁₋₃B). Expression of hybrid chimeras with XL LuxB replaced by *P. phosphoreum* (PP) or *P. leiognathi* (PL) LuxB subunits decreased luminescence by at least 15-fold. Therefore, only the active chimeras with XL LuxB (LuxA₁B, LuxA₂B, and LuxA₃B) were extracted from the cells and investigated further.

Thermal Stabilities of Chimeric Luciferases. The thermal stabilities of XL and PP luciferase are remarkably different. At 35°C , XL luciferase is completely stable while PP

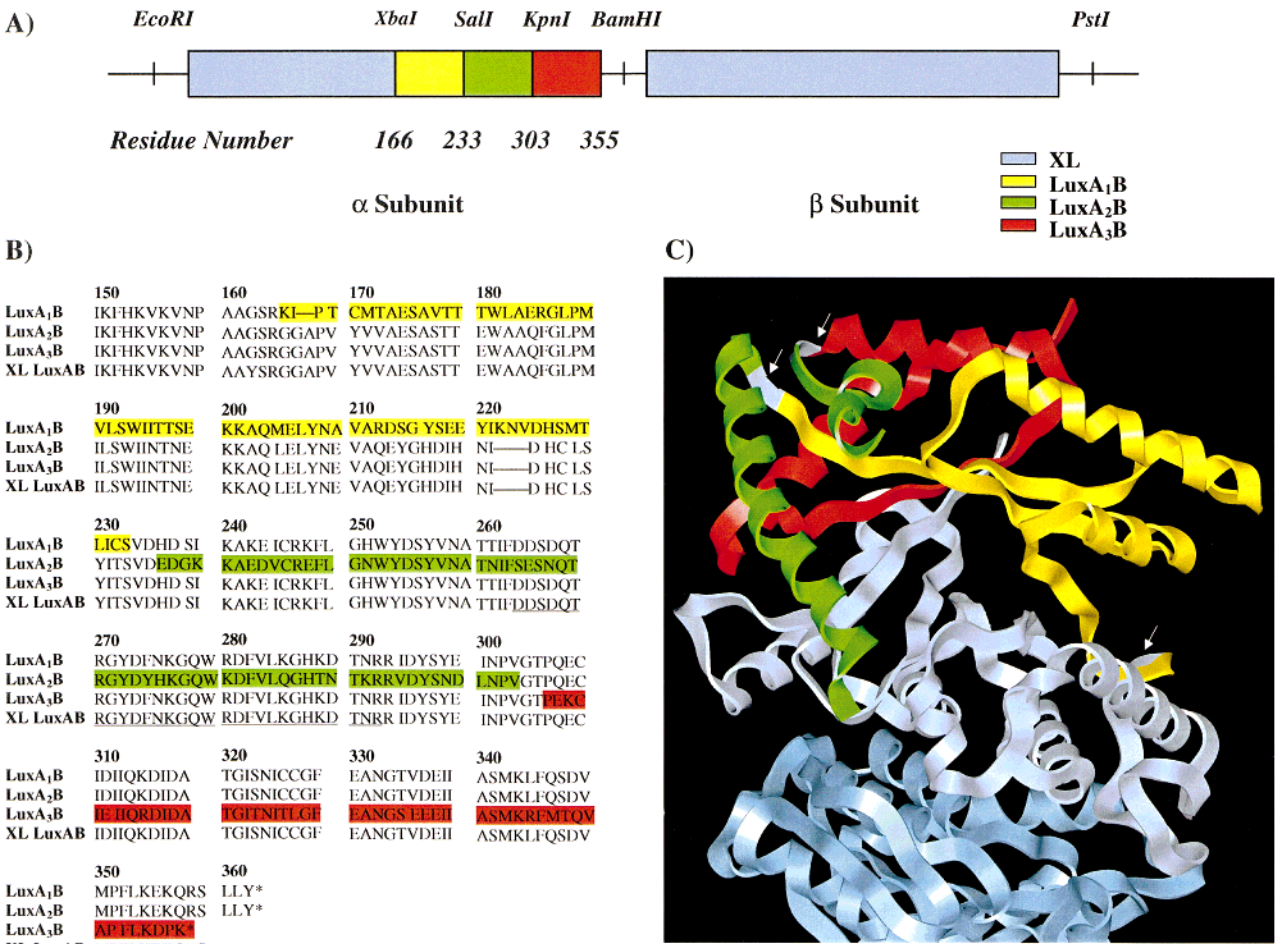


FIGURE 2: Structural representations of the chimeric luciferases. (A) Restriction diagram illustrating the construction of the chimeric luciferases. The restriction sites for *XbaI*, *Sall*, and *KpnI* were introduced into the second half of the α subunit of XL luciferase at the residues indicated. The chimeric α subunits were generated by substituting the equivalent regions from *P. phosphoreum* into the appropriate restriction sites. The chimeras thus generated are referred to as LuxA₁B, LuxA₂B, and LuxA₃B. (B) Sequence alignment of the LuxA₁B (yellow), LuxA₂B (green), and LuxA₃B (red) chimeras with the sequence of the native XL LuxAB. The colored portions represent the substituted sequence of PP luciferase in XL LuxAB. The protease-sensitive loop is underlined. (C) Three-dimensional structure of the luciferase from *Vibrio harveyi* used as a representative model of the chimeric luciferases. The portions in yellow (LuxA₁B), green (LuxA₂B), and red (LuxA₃B) represent the parts of the molecule originating from *P. phosphoreum* in each respective chimera. The arrows denote the location of the restriction sites used in the construction of the chimeras.

luciferase is inactivated at a rate of 1.8 min⁻¹ (Figure 3). Indeed, *P. phosphoreum* species are generally found at colder temperatures in mid to deep waters of the ocean while *X. luminescens* is terrestrial, living in nematodes and insects (25, 26). Analysis of the thermal stabilities of the chimeras at 35 °C showed that the LuxA₁B chimera had become almost as labile as PP luciferase (2.7 min⁻¹) while the LuxA₂B and LuxA₃B chimeras remained very stable with rate constants for inactivation at 35 °C over 300-fold lower than that for PP luciferase.

Dependence of the Decay Rate of Luminescence on Aldehyde Chain Length. The decay rates of luminescence for the parental and chimeric luciferases with dodecanal are compared in Figure 4. As free FMNH₂ is chemically oxidized in the first second of this assay, the initial maximum in luminescence [*I*(0)] due to the enzyme-flavin complex decays exponentially with time [*I*(*t*)]. LuxA₃B and LuxA₂B have rate constants for luminescence decay of 0.028 and 0.035 s⁻¹, respectively, very similar to the rate constant for decay of the parental XL luciferase (0.027 s⁻¹). The rate constant for luminescence decay of the chimera LuxA₁B (0.077 s⁻¹) is much more rapid and comparable to that of

Table 1: Luminescence of *E. coli* Cells Containing Chimeric Luciferases^a

luciferase	α subunit	β subunit	% activity ^b
LuxAB	XL	XL	100
LuxAB _{PP}	XL	PP	38
LuxAB _{PL}	XL	PL	0.03
LuxA ₁ B	XL- Δ PP ₁	XL	0.03
LuxA ₁ B _{PP}	XL- Δ PP ₁	PP	—
LuxA ₁ B _{PL}	XL- Δ PP ₁	PL	—
LuxA ₂ B	XL- Δ PP ₂	XL	31
LuxA ₂ B _{PP}	XL- Δ PP ₂	PP	2
LuxA ₂ B _{PL}	XL- Δ PP ₂	PL	—
LuxA ₃ B	XL- Δ PP ₃	XL	9
LuxA ₃ B _{PP}	XL- Δ PP ₃	PP	0.3
LuxA ₃ B _{PL}	XL- Δ PP ₃	PL	—
LuxA ₁₋₃ B	XL- Δ PP ₁₋₃	XL	—

^a XL, *Xenorhabdus luminescens*; PP, *Photobacterium phosphoreum*; PL, *Photobacterium leiognathi*. Segments of PP luciferase inserted in the XL α subunit are indicated by Δ PP with the adjoining numbers corresponding to the regions depicted in Figure 2. ^b In vivo luminescence of 1 mL of *E. coli* cells containing the respective luciferases grown at 30 °C to an OD_{660 nm} of 2.5 or greater. The activity is expressed as LU/OD_{660 nm}; the control LuxAB had an activity of 2.6 LU/OD_{660 nm}. (—) Luminescence activity not detected.

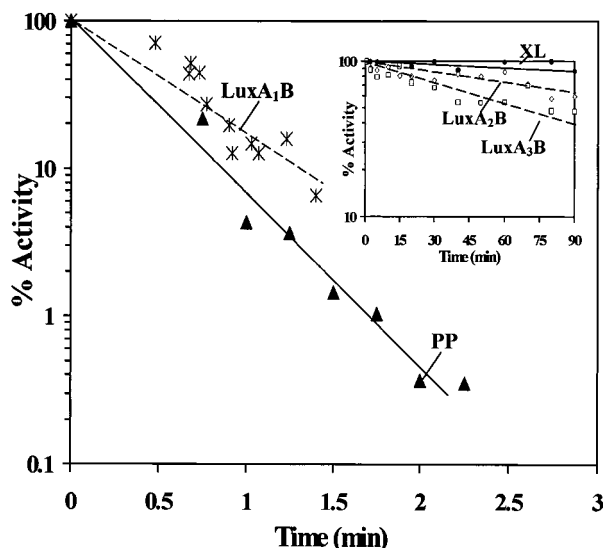


FIGURE 3: Thermal stabilities of the chimeric and parental luciferases. The luciferases were incubated in 50 mM phosphate, pH 7, containing 20 mM β -mercaptoethanol at 35 °C and aliquots assayed with time. The PP luciferase and LuxA₁B are remarkably similar with an inactivation half-time of less than 30 s. In contrast (inset), the parental XL luciferase, LuxA₂B, and LuxA₃B all show greatly improved thermostabilities.

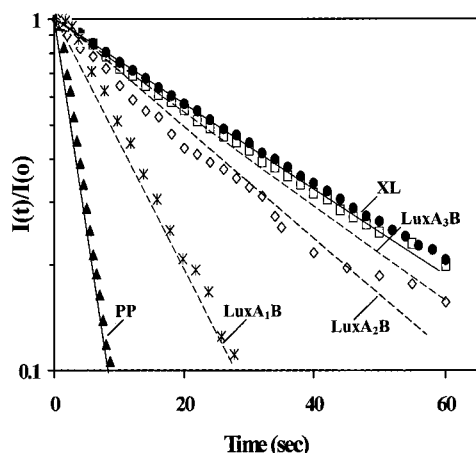


FIGURE 4: Decay of luminescence of the native *X. luminescens* and *P. phosphoreum* luciferases and of the three chimeric luciferases LuxA₁B, LuxA₂B, and LuxA₃B with dodecanal, using the standard assay. The native XL luciferase and the chimera LuxA₃B have the slowest decay rates while the native PP luciferase and the chimera LuxA₁B show markedly faster turnover rates. The chimera LuxA₂B has an intermediate rate of decay.

PP luciferase (0.26 s^{-1}), implicating the region substituted with PP LuxA (residues 166–233) in controlling the decay of the EFOA intermediate and light emission. Further support for this conclusion was obtained by measuring the decay rates of the chimeras with other fatty aldehyde substrates (Figure 5). The rate constants for luminescence decay for LuxA₁B with octanal, nonanal, decanal, and undecanal closely parallel the corresponding rate constants for PP luciferase. In contrast, the rate constants for the other two chimeras, LuxA₂B and LuxA₃B, are similar to those for the parental XL luciferase. Interestingly, the substituted region in the chimera, LuxA₃B, has resulted in slower rates of luminescence decay for nonanal, decanal, and undecanal than the corresponding decay rates for XL luciferase and generated a luciferase with decay rates relatively independent of aldehyde chain length.

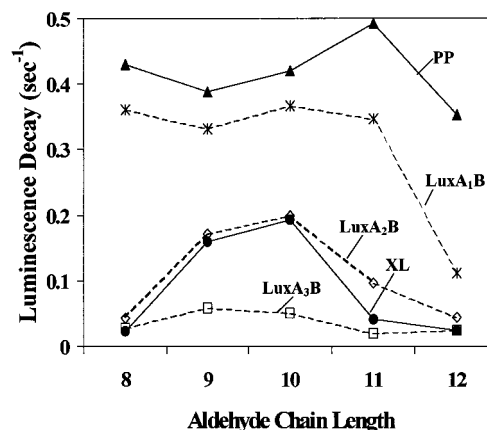


FIGURE 5: Decay rates of luminescence as a function of aldehyde chain length. The rate of decay for XL luciferase is similar to that of the chimera LuxA₂B, and comparable to that of the chimera LuxA₃B. The decay rates for PP luciferase and LuxA₁B are much faster than the other three enzymes. The decay rates were determined with the standard assay.

Specific Activities and Quantum Yields as a Function of Aldehyde Chain Length. As both LuxA₂B and LuxA₃B were stable and had good activity in extracts, these chimeras could be purified to homogeneity. Table 2 gives the specific activities and quantum efficiencies with different aldehydes; LuxA₂B had 34–76% of the specific activity and 20–46% of the quantum yield while LuxA₃B had 7–30% of the specific activity and 15–32% of the quantum yield of XL luciferase depending on the aldehyde chain length. These results indicate that the catalytic efficiency on replacement of a large number of amino acid residues in the carboxyl-terminal regions is not compromised to a large extent. The lower specific activities (7–10%) with nonanal, decanal, and undecanal for LuxA₃B but the higher quantum yields (20–25%) compared to those with XL can be directly correlated with the differences in decay rates between XL luciferase and LuxA₃B noted in Figure 5.

Dependence of the Decay Rate of Luminescence on Aldehyde Concentration. The responses of the chimeric luciferases to increasing decanal concentrations are shown in Figure 6. The parent XL luciferase and the chimeras LuxA₂B and LuxA₃B show maximum activity between 10 and 30 μM decanal although the latter chimera has a weaker response at lower aldehyde concentrations than the other two luciferases (Figure 6A). In contrast, the remaining chimera, LuxA₁B, and PP luciferase require higher aldehyde concentrations for maximum activity (~ 100 and 250 μM , respectively), and inhibition of activity occurs at much higher decanal concentrations. The dependence of the rates of luminescence decay on decanal concentration is shown in Figure 6B. The decay rates for the parental XL luciferase and the LuxA₂B chimera are very similar, increasing at higher decanal concentrations and contrasting sharply with those of PP luciferase. The rate of luminescence decay for LuxA₃B is slower and only shows a small increase in decay rate with increasing decanal concentration. In sharp contrast, the LuxA₁B chimera shows a remarkably similar pattern to PP luciferase with the decay rate decreasing at high aldehyde concentrations. Particularly noteworthy is that the decay rate of the “fast” PP luciferase is actually lower than that of the “slow” XL luciferase at high decanal concentrations.

Table 2: Specific Activities and Quantum Yields of the Purified Chimeras LuxA₂B and LuxA₃B as a Function of Aldehyde Chain Length

aldehyde chain length	LuxA ₂ B		LuxA ₃ B	
	specific activity ^a	quantum yield ^b	specific activity	quantum yield
8	5.8×10^{12} (45) ^c	9.3×10^{13} (24)	2.3×10^{12} (18)	5.9×10^{13} (15)
9	4.5×10^{13} (50)	1.8×10^{14} (46)	7.7×10^{12} (8)	9.2×10^{13} (24)
10	4.8×10^{13} (44)	1.7×10^{14} (44)	7.3×10^{12} (7)	9.9×10^{13} (25)
11	1.6×10^{13} (76)	1.2×10^{14} (34)	2.0×10^{12} (10)	7.0×10^{13} (20)
12	4.8×10^{12} (34)	7.6×10^{13} (20)	4.2×10^{12} (30)	1.2×10^{14} (32)

^a The specific activities of XL luciferase with octanal, nonanal, decanal, undecanal, and dodecanal were 1.3×10^{13} , 9.1×10^{13} , 1.1×10^{14} , 2.1×10^{13} , and 1.4×10^{13} quanta s⁻¹ mg⁻¹. ^b The total quantum yields of XL luciferase with octanal, nonanal, decanal, undecanal, and dodecanal were 3.9×10^{14} , 3.9×10^{14} , 3.9×10^{14} , 3.5×10^{14} , and 3.8×10^{14} quanta mg⁻¹. ^c The numbers in parentheses represent percentages relative to XL luciferase with the same aldehyde.

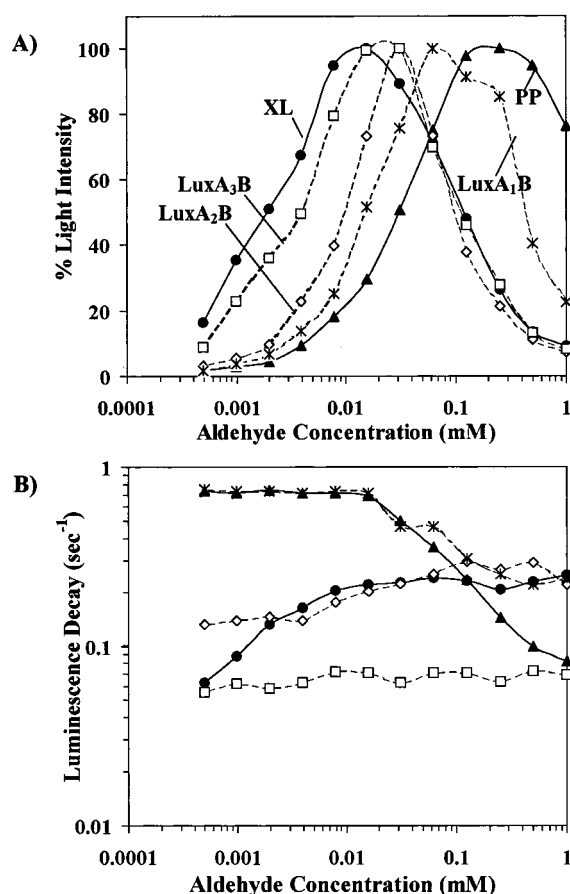


FIGURE 6: Dependence of the intensity and decay rate of luminescence on decanal concentration. (A) Dependence of the maximum luminescence $[I(o)]$ on decanal concentration. The native luciferase XL and the two chimeric luciferases LuxA₂B and LuxA₃B have optimal responses at 0.1–0.3 mM decanal and are inhibited at concentrations above 50 μ M, and differ markedly from the responses of the PP luciferase and from the chimera LuxA₁B. (B) Dependence of the decay rates of luminescence on decanal concentration. The decay rate of XL luciferase is intermediate between those of LuxA₂B and LuxA₃B, with higher rates at increasing decanal concentrations. The decay rates of PP luciferase and LuxA₁B are markedly higher at low aldehyde concentrations and decrease at high decanal concentrations.

The first-order decay of luminescence in these experiments is directly related to the decay of the EFOA intermediate. Consequently, the rate constant for luminescence decay (k_T) can be related to the rate constants for decay (k_L and k_D) for the light and dark pathways (see Figure 1) by the equation:

$$k_T = (k_L A + k_D K_a) / (K_a + A)$$

where K_a is the dissociation constant for the aldehyde, A .

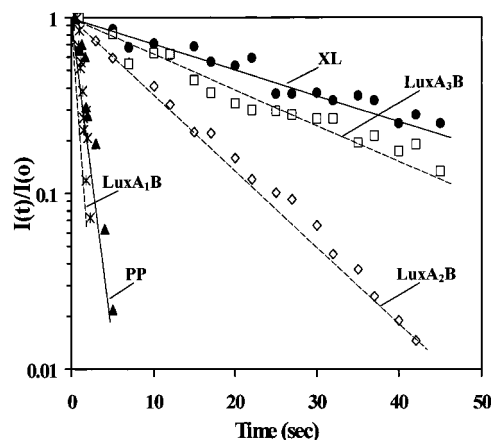


FIGURE 7: Decay rates of the EFO intermediates of parental and chimeric luciferases. The decay rates of the EFO intermediate of PP luciferase and LuxA₁B are very rapid relative to those of XL luciferase, LuxA₂B, and LuxA₃B. The assay was carried out by the injection of 1 mL of 50 μ M catalytically reduced FMNH₂ into a 1 mL mixture of the enzyme in 50 mM phosphate buffer with 0.2% BSA, and 1 mL of 0.001% decanal was injected at subsequently timed intervals.

The derivation of this equation presumes that the decay rate constants (k_L and k_D) are much smaller than the rate constants for the binding and release of aldehyde, a reasonable assumption in view of the very slow turnover of the enzyme. Under these conditions, the rate constant for decay of luminescence, k_T , should remain close to first order at all aldehyde concentrations, a result consistent with experimental observations. At high aldehyde concentrations ($A \gg K_a$), $k_T = k_L$, and at low aldehyde concentrations ($K_a \ll A$), $k_T = k_D$ with $K_a = A$ when $k_T = (k_D + k_L)/2$. Consequently, the EFOA complex decays primarily via EFO without emission of light at low aldehyde concentration and via the excited state at high aldehyde concentration. A relatively constant decay rate with changing aldehyde concentration for a chimera would suggest that k_D and k_L must be of similar magnitude for this luciferase and a particular aldehyde.

Decay of the EFO Enzyme Intermediate. As a measure of the validity of the above equation, the decay rate of the intermediate enzyme–flavin complex EFO formed prior to aldehyde binding was directly measured (Figure 7). The decay rates for the EFO complex (k_D) of PP luciferase (0.64 s⁻¹) and LuxA₁B (0.82 s⁻¹) are very similar and much higher than the decay rate for the EFO complex of XL luciferase (0.032 s⁻¹). In contrast, the decay rates of the EFO complex for the chimeras LuxA₂B (0.097 s⁻¹) and LuxA₃B (0.045 s⁻¹) are much more closely related to that of the parental XL luciferase. These values agree closely with the rate

Table 3: Activity with Flavin Analogues

luciferase	% activity ^a		
	carboxypentylflavin	riboflavin	riboflavin + 0.8 M SO ₄ ²⁻
XL	60	4	25
PP	0.4	<0.3	<0.2
LuxA ₁ B	1	3	11
LuxA ₂ B	9	0.05	1
LuxA ₃ B	27	0.2	4

^a Activities were measured as the maximum light intensity in the dithionite assay on injection of 1.0 mL of 0.01% decanal into phosphate buffer, pH 7.0, containing 50 μ M reduced flavin and are reported as percentage of the activity with FMNH₂.

constants measured for EFOA decay at very low decanal concentration (Figure 6B), i.e., ~ 0.05 s⁻¹ for XL luciferase and LuxA₃B, 0.13 s⁻¹ for LuxA₂B, and 0.75 s⁻¹ for both PP luciferase and LuxA₁B. This result explains why the turnover rate (k_T) for luminescence at different decanal concentrations for LuxA₃B is constant as k_D and k_L have very similar values (0.05 s⁻¹). This equation also provides a valid description of luminescence decay even at nonsaturating aldehyde concentrations and allows measurements of not only k_D and k_L but also K_a .

Flavin Specificity and Interactions. The XL and PP luciferases differ considerably in their abilities to function with FMNH₂ analogues. The XL luciferase has reasonably good activity (4–60%) with both reduced carboxypentylflavin and riboflavin while PP luciferase has very low activity with these FMN analogues (<0.4%) compared to that with FMNH₂ (Table 3). Two of the chimeras, LuxA₂B and LuxA₃B, retained a reasonable level of activity with reduced carboxypentylflavin (9–27%) but have very low activities with riboflavin (0.05–0.2%). In contrast, the LuxA₁B chimera had relatively high activity with riboflavin and low activity with carboxypentylflavin. The differential activities of the chimeras with the flavin analogues suggest that residues close to the carboxyl terminal of LuxA are important for interaction with the flavin ring while the negatively charged groups on carboxypentylflavin and FMN bind outside this region. A large stimulation (10–20-fold) of activity of LuxA₂B and LuxA₃B with riboflavin by the sulfate dianion (Table 3), which can act in an autosteric manner with riboflavin to partially mimic FMN (27), can readily be observed. This stimulatory effect by sulfate occurs with XL but not PP luciferase (Table 3). The activity of the LuxA₁B chimera with riboflavin is stimulated to a lesser degree by sulfate (<4-fold), indicating that this region might be partially involved in binding the negatively charged moiety.

To analyze the interactions with flavin more directly, the dissociation constants (K_d) for FMNH₂ and reduced carboxypentylflavin were measured in the dithionite assay. Table 4 shows that the K_d s for FMNH₂ were similar for XL LuxAB and PP LuxAB as well as the chimera LuxA₁B. In contrast, the chimeras LuxA₂B and LuxA₃B had much higher dissociation constants for FMNH₂, indicating again that the carboxyl-terminal region interacted with flavin. Similar results were obtained with reduced carboxypentylflavin, with both LuxA₂B and LuxA₃B having higher flavin dissociation constants than that of XL luciferase. Dissociation constants could not be measured for reduced carboxypentylflavin for PP luciferase or the chimera LuxA₁B due to their low activities with this flavin analogue compared to FMNH₂.

Table 4: Dissociation Constants for FMNH₂ and Reduced Carboxypentylflavin

luciferase	K_d^a (FMNH ₂) (μ M)	K_d (COO–FMNH ₂) (μ M)
XL	1.4	1.1
PP	1.3	— ^b
LuxA ₁ B	1.7	— ^b
LuxA ₂ B	7	4
LuxA ₃ B	11	23

^a All the reported K_d 's were determined by curve fitting with the software Enzfitter. ^b Not measured due to low enzymatic activity.

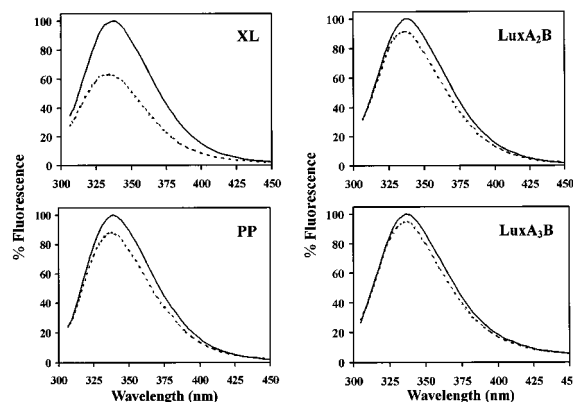


FIGURE 8: Fluorescence spectra of the native and chimeric luciferases showing their different affinities for FMN. The native enzymes alone (solid lines) give approximately the same fluorescence yield and are normalized to 100%. The addition of 10 μ M FMN in the presence of 50 μ M myristic acid (dotted lines) quenches the fluorescence of XL luciferase to a much greater extent than that of the other luciferases. The protein concentration was 2 μ M, and the enzymes were buffered in 50 mM phosphate, pH 7, and 20 mM β -mercaptoethanol.

To investigate the interactions of LuxA₂B and LuxA₃B with flavin directly, the quenching of the intrinsic fluorescence of the purified chimeric and parental luciferases by FMN was compared. Figure 8 shows the emission spectra of the luciferases are very similar and that the quenching by FMN is much weaker for the chimeras and the PP luciferase than the parental XL luciferase. The fluorescence of XL luciferase is quenched by 40% by FMN while the fluorescence of chimera LuxA₂B and PP luciferase are quenched to the same extent (10%) with the LuxA₃B chimera being quenched the least (5%). The lower extent of quenching reflects a weaker binding of FMN as the quenching of PP luciferase and the two chimeras can be increased by adding higher concentrations of FMN. Calculation of the dissociation constants for FMN from the fluorescence quenching at different FMN concentrations showed that the K_d (FMN) values for LuxA₂B and LuxA₃B were substantially higher (30 μ M and 80 μ M, respectively) than that for XL luciferase (4 μ M) and quite similar to that for PP luciferase (40 μ M). This result shows that flavin interactions are weakened in both the LuxA₂B and LuxA₃B chimeras.

DISCUSSION

Previous work on bacterial luciferase (19, 28) has established that the catalytic properties are primarily dictated by the LuxA subunit in the heterodimeric enzyme (LuxAB). Hybrid luciferases containing subunits from different species have been shown to have catalytic properties almost identical to the parental luciferase containing the same LuxA subunit

(20, 29) even though the LuxB subunits could differ in amino acid sequence at well over 100 positions. The generation of luciferases with chimeric LuxA subunits provides an alternate approach with the potential of defining the region within LuxA containing the key residues controlling the catalytic properties. This approach is useful as specific residues or regions in LuxA have not yet been implicated in the chemical mechanism for the light-emitting reaction (26, 30) and luciferase with bound substrates has not been crystallized (4).

The crystal structure of luciferase shows that both the LuxA and LuxB subunits are eight-stranded α/β barrels (3, 4). Close subunit contacts occur between the α_2 and α_3 helices in each subunit as well as with hairpin loops between the α_4 helix and β_5 strand in both subunits which lie at the subunit interface. To avoid disruption of the subunit contacts, chimeric *X. luminescens* LuxA subunits were generated by replacing segments of the last half of the eight-stranded β/α barrel with sequences from *P. phosphoreum* LuxA, whose sequence and enzymatic and physical properties have extensively diverged from those of *X. luminescens* luciferase. Three chimeric luciferases were generated: the chimera LuxA₁B had the β_5 - α_5 - β_6 - α_6 - β_7 region replaced; the chimera LuxA₂B had a 71 amino acid loop between the β_7 strand and the α_7 helix replaced; and the chimera LuxA₃B had the carboxyl-terminal α_7 - β_8 - α_8 segment replaced. The sequence in the loop region replaced in LuxA₂B is composed of an α -helix, α_{7a} , and a β -strand, β_{7b} , flanking a disordered region that can be protected from proteolytic cleavage by FMNH₂ (3, 5).

Despite substitution of about one-sixth of the sequence of XL LuxA by PP LuxA in LuxA₂B and LuxA₃B, these chimeras retained properties very comparable to those of XL luciferase including thermal stability, decay rates via both light and dark pathways, and dependence of activity on type and concentration of fatty aldehyde. The most distinct changes in the properties of these two chimeras were a decrease in interactions with both oxidized and reduced flavins and a relative loss of activity with riboflavin. However, the activities with riboflavin for both LuxA₂B and LuxA₃B could be strongly stimulated by exogenous sulfate, which partially replaces the phosphate missing in riboflavin but present in FMN (27). This result suggests that the region involved in binding the phosphate of FMNH₂ is not located in the carboxyl-terminal regions as sulfate does not stimulate the activity of PP luciferase with riboflavin. Although the phosphate binding site for FMN is located near the loops connecting the last two β - α units for most (β/α)₈ barrel flavoenzymes, such as glycolate oxidase, flavocytochrome *b*₂, and trimethylamine dehydrogenase (31–33), the crystallographic data for *V. harveyi* luciferase indicated that an electron-dense site in the region of the β_5 - α_5 loop was the phosphate binding site (4). Even though the substituted region in LuxA₁B encompasses the β_5 - α_5 loop, sulfate can still stimulate to some degree the activity of LuxA₁B with riboflavin, suggesting binding contributions by residues outside this region. These results do indicate, however, that the carboxyl-terminal regions in the last one-third of LuxA affect the binding of flavin by interacting with the flavin ring of FMN and not with the phosphate residue. Moreover, the key residues involved in controlling turnover and properties defining “slow” and “fast” decay luciferases are

located outside the LuxA carboxyl-terminal regions.

The properties of the third chimera, LuxA₁B, were remarkably different from the other two chimeras and surprisingly, in many aspects, closely resembled the properties of PP luciferase even though over 90% of the chimera (or 80% of LuxA) was composed of XL luciferase. The most notable property of LuxA₁B was its rapid rate of luminescence decay compared to that of XL luciferase. The fast decay rate arose from a low aldehyde binding affinity and a rapid rate of decay of the EFO complex via a dark pathway. Both these latter properties of LuxA₁B closely paralleled the same properties of PP luciferase. Indeed, the rate of decay of luminescence at low decanal concentration could be equated to the rate constant for decay of decomposition of EFO by a dark pathway. The difference between the fast luminescence decay with PP luciferase or LuxA₁B, on one hand, and the slow decay of XL luciferase, LuxA₂B, and LuxA₃B with decanal, on the other, indicates that the substituted region in LuxA₁B encompasses the key residues (166–203 of LuxA) involved in aldehyde binding and the mechanism of turnover of the EFO and EFOA intermediates. A striking similarity between the luminescence decay rates of LuxA₁B and PP luciferase with aldehydes of different chain length greatly strengthened this conclusion.

Analyses of the thermal stabilities also showed that the LuxA₁B chimera and PP luciferase had very similar properties with the inactivation rates at 35 °C being very rapid and over 300 times faster than those for chimeras LuxA₂B and LuxA₃B. Interestingly, both sets of properties (thermal lability and “fast” decay rates) are characteristic of luciferases from the *Photobacterium* genus while thermal stability and “slow” decay rates are characteristic of luciferases from the *Xenorhabdus* (*Photorhabdus*) genus and *V. harveyi* species. Although there were major changes in most properties for the LuxA₁B, changes directly related to flavin binding were much less pronounced. In particular, the *K*_d for FMNH₂ remained low for the LuxA₁B chimera, and its ability to function with riboflavin was much better than the other two chimeras.

These results have thus implicated the carboxyl-terminal regions extending from the end of the β_7 strand through the flexible loop to the carboxyl-terminal of LuxA in interaction with the flavin ring. In contrast, the central region extending through the β_5 - α_5 - β_6 - α_6 - β_7 region controlled the interactions with different aldehydes as well as the decay of the EFO and EFOA intermediates. The differences in amino acid sequence in the central region between the “slow” XL luciferase and the “fast” PP luciferase appear to be the primary reason for luciferases being classed into two major groups with different decay rates.

REFERENCES

1. Hastings, J. W., and Gibson, Q. H. (1963) *J. Biol. Chem.* 238, 2537–2554.
2. Gibson, Q. H., and Hastings, J. W. (1962) *Biochem. J.* 83, 368–377.
3. Fisher, A. J., Thompson, T. B., Thoden, J. B., Baldwin, T. O., and Rayment I. (1996) *J. Biol. Chem.* 271, 21956–21968.
4. Fisher, A. J., Raushel, F. M., Baldwin, T. O., and Rayment, I. (1995) *Biochemistry* 34, 6581–6586.
5. Aboukhaire, N. K., Ziegler, M. M., and Baldwin, T. O. (1985) *Biochemistry* 24, 3942–3947.

6. Li, Z., and Meighen E. A. (1995) *Biochemistry* 34, 15084–15090.
7. Farber, G. K., and Petsko, G. A. (1990) *Trends Biochem. Sci.* 15, 228–234.
8. Nealsen, K. H. (1978) *Methods Enzymol.* 57, 153–166.
9. Nealsen, K. H., and Hastings, J. W. (1979) *Microbiol. Rev.* 43, 496–518.
10. Schmidt, T. M., Kopecky, K., and Nealsen, K. H. (1989) *Appl. Environ. Microbiol.* 55, 2607–2612.
11. Szittner, R., and Meighen, E. A. (1990) *J. Biol. Chem.* 265, 16581–16587.
12. Li, Z., Szittner, R., and Meighen, E. A. (1993) *Biochim. Biophys. Acta* 1158, 137–145.
13. Bohren, K. M., Grimshaw, C. E., and Gabbay, K. H. (1992) *J. Biol. Chem.* 267, 20965–20970.
14. Osterman, A. L., Lueder, D. V., Quick, M., Myers, D., Canagarajah, B. J., and Phillips, M. A. (1995) *Biochemistry* 34, 13431–13436.
15. Tsugeno, Y., Hirashiki, I., Ogata, F., and Ito, A. (1995) *J. Biochem. (Tokyo)* 118, 974–980.
16. Nandy, A., Kieweg, V., Kräutle, F. G., Vock, P., Küchler, B., Bross, P., Kim, J. J., Rasched, I., and Ghisla, S. (1996) *Biochemistry* 35, 12402–12411.
17. Murata, L. B., and Schachman, H. K. (1996) *Protein Sci.* 5, 4719–4728.
18. Meighen, E. A., and Hastings, J. W. (1971) *J. Biol. Chem.* 246, 7666–7674.
19. Cline, T. W., and Hastings, J. W. (1972) *Biochemistry* 11, 3359–3370.
20. Ruby, E. G., and Hastings, J. W. (1980) *Biochemistry* 19, 4989–4993.
21. Tabor, S., and Richardson, C. C. (1985) *Proc. Natl. Acad. Sci. U.S.A.* 82, 1074–1078.
22. Gunsalus-Miguel, A., Meighen, E. A., Nicoli, M. Z., Nealsen, K. H., and Hastings, J. W. (1972) *J. Biol. Chem.* 247, 398–404.
23. Hastings, J. W., and Weber, G. (1963) *J. Opt. Soc. Am.* 53, 1410–1415.
24. Lackowicz, J. R. (1983) *Principles of Fluorescence Spectroscopy*, Plenum Press, New York.
25. Poinar, G. O., Haygood, T. G., and Nealsen, K. H. (1980) *Soil Biol. Biochem.* 12, 5–10.
26. Meighen, E. A., and Dunlap, P. V. (1993) *Adv. Microb. Physiol.* 34, 1–67.
27. Meighen, E. A., and MacKenzie R. E. (1973) *Biochemistry* 12, 1482–1491.
28. Meighen, E. A., Nicoli, M. Z., and Hastings, J. W. (1971) *Biochemistry* 10, 4069–4073.
29. Bartlet, I., and Meighen, E. A. (1980) *J. Biol. Chem.* 255, 11181–11187.
30. Baldwin, T. O., and Ziegler, M. M (1992) in *Chemistry and Biochemistry of Flavoenzymes* (Muller, F., Ed.) pp 467–530, CRC Press, Boca Raton.
31. Lindqvist, Y. (1989) *J. Mol. Biol.* 209, 151–166.
32. Xia, Z.-X., and Mathews, F. S. (1990) *J. Mol. Biol.* 212, 837–863.
33. Lim, L. W., Shamala, N., Mathews, F. S., Steenkamp, D. J., Hamlin, R., and Xuong, N. H. (1986) *J. Biol. Chem.* 261, 15140–15146.

BI991407N